Polyethylene diblock copolymers: direct synthesis and morphological analysis*

M. A. Drzewinski
*EniChem America, Inc., Corporate Research and Development Center,
Monmouth Junction, NJ 08852, USA*

A variety of diblock copolymers containing a high density polyethylene block were synthesized directly by a transformation reaction from an anionic to a Ziegler–Natta type polymerization. A wide range of reaction parameters were investigated and optimized. Efficiencies of conversion of the anionic first block to diblock were as high as 33% (100% normalized), consistent with the known 3/1 Li-R/Ti relationship in the active catalyst species. The activity of the polymeric Li-R/Ti catalyst with regards to ethylene polymerization was as high as 40 000 g of polymer per mole Ti. Molecular characterization of the resultant polymers is consistent with diblock copolymer structures, especially the characteristic microphase-separated structure exhibited in transmission electron micrographs. Detailed microscopic and X-ray analyses show distinct differences, however, between the morphological behaviour of these materials and the now well established morphological behaviour of amorphous–amorphous diblock copolymers. These differences are readily explained by consideration of the interactions between the competing thermodynamic processes of microphase separation and crystallization in these copolymers.

(Keywords: diblock copolymers; synthesis; morphology)

INTRODUCTION

The unique mechanical behaviour and strong interfacial activity demonstrated by block copolymers has been the main driving force behind research in our laboratory. The development of well defined block copolymers, however, is somewhat restricted by the nature of synthesis. For this reason the best characterized and most studied systems have been those made by anionic synthesis. The range of monomers amenable to this type of synthesis is limited, such that the advantageous properties of crystalline polyolefins (e.g. heat and solvent resistance) are not realized in block copolymers. Therefore, over the past few years we have developed means by which to synthesize well defined block copolymers containing a semicrystalline polyolefin so as to overcome many of the deficiencies of purely amorphous hydrocarbon block copolymers.

Although Ziegler–Natta (ZN) catalysis is the prevalent method for the synthesis of polyolefins, it has very limited application in block copolymers owing to the short active lifetimes of the growing polymer chains. In most cases, claims of polyolefin block copolymer formation with ZN systems have not been proven directly but instead inferred from physical properties and the method of synthesis[1–3]. However, experimental evidence has shown that many of these commercial claims are indeed nothing more than intimate blends of homopolymers which show enhanced properties due to the fine level of dispersion achieved by *in situ* polymerization[4,5]. This is not to say that olefinic block copolymers have never been made with ZN-type catalysis but instead that the resultant product is most likely an intimate mixture of homopolymers, random/tapered copolymers and perhaps some block copolymer. The yield for production of ZN-synthesized polyolefin diblock copolymers has been estimated to be, at best, $\ll 20\%$ based on measured lifetimes of the growing chains[6].

By understanding the basic requirements for block copolymer formation and the nature of various polymerization mechanisms, one can successfully polymerize relatively well defined polyolefin diblock copolymers using a transformation reaction from anionic to ZN catalysis. A brief description of this reaction and its optimization to produce polyethylene containing diblocks of predetermined composition is given below. In addition, the behaviour of these resultant diblock copolymers has been characterized and explained in terms of the morphological hierarchy that occurs. The morphological hierarchy, however, is more complex than that known for amorphous–amorphous diblocks and arises from the competition between the thermodynamically driven and kinetically controlled processes of microphase separation and crystallization. A qualitative explanation for the resultant morphological hierarchy in these systems is also described below.

Motivation for this work

Recently there has been a renewed interest in polyolefin blends and so work in our laboratory once again turned to the study of the synthesis of polyolefin block copolymers, particularly those based on polyethylene.

---

* Presented at the American Chemical Society, Division of Polymer Chemistry '17th Biennial Symposium on Advances in Polymerization and High Performance Polymeric Materials', 22–25 November 1992, Palm Springs, CA, USA

0032-3861/94/23/5024–11

This new work has focused on understanding the chemistry of the catalyst in order to best optimize and control the overall composition of the blocks. From studies of the mechanical behaviour of the earlier materials it became apparent that variations in the block composition and sample preparation could produce wide variations in properties. These variations in properties appear much greater than those typically found in amorphous block copolymers and arise from the coexistence of the microphase-separated block copolymer structure and the semicrystalline morphology in the polyolefin block.

In the case of a crystallizable diblock copolymer, the processes of microphase separation and crystallization should be expected to be interrelated. The usual constraints of the block copolymer (reduced chain ends, limited conformations, formation of surfaces and junction points located at or near the interface) could all contribute to affecting the local free energy of the crystallizable block. Thus, one could presuppose that the formation of the surfaces in the melt (i.e. microphase separation) should have an effect on the nature of crystallization of the crystallizable block for energetic reasons. Furthermore, if one presupposes that microphase separation in the melt acts to eliminate chain ends, align crystallizable chains at a common surface and in turn lower the local free energy at the surface, then one would expect chain folding to be promoted and to occur such that the chain axis is parallel to the surface for minimization of the free energy. Such a situation is analogous to epitaxial growth on an oriented polymer surface and is referred to as orientation-induced nucleation[7,8]. The effects of block copolymerization on the energetics of crystallization, as well as the proposal of chain growth parallel to the microphase-separated surface, have been reported previously[9,10] and, very recently, verified morphologically[11-14].

In order to properly evaluate these morphological effects it became necessary to gain control over the polymerization in order to produce specific structures and resultant behaviour. Although the anionic to ZN transformation reaction has been reported previously[9,15-21], optimization and further development to produce specific diblock structures has not. In order to do this, a better understanding of the factors that affect the transformation was required. The many factors that affect anion[22] or ZN catalyst systems[6,9] have been published previously. In addition, a fair amount of literature has existed for some time regarding the polymerization ability of a catalyst produced from n-butyl lithium (n-BuLi) and titanium tetrachloride ($TiCl_4$). Thus, it would seem quite apparent that substitution of a living anionic polymer for the n-BuLi should produce similar results. This idea is consistent with the premise of chain length independence in polymerization reactions[23] and the fact that the alkylating species of the ZN complex has been shown to become the end group in the resultant polymer[24-33]. Optimization of the reaction, however, is not so straightforward. In order to do this, more information needed to be gathered on how the various reaction parameters affect not only the 'activity' with regard to polymerizing polyethylene, but also the 'efficiency' of transforming the first block into diblock copolymer. Only when both are optimized simultaneously can one achieve high yields of diblock copolymer with a specified composition. Recent synthetic studies have therefore concentrated on the n-BuLi/$TiCl_4$ system, and have confirmed many earlier observations[34-52]. In addition, new characteristics important to the polybutadienyl lithium/$TiCl_4$ system, which were not properly explained in the more recent work[15-19,53-58], have been identified.

Therefore, this paper presents not only the findings of the synthetic investigations but also provides evidence for the influence of block copolymer microphase separation on the crystallization process as well as the resultant morphological hierarchy that is achieved as a result of the coexistence of these two phenomena.

EXPERIMENTAL

Homopolymer synthesis

In order to best optimize the block copolymerization reactions, homopolymerizations of polyethylene were carried out using a catalyst system of n-BuLi/$TiCl_4$ under a variety of conditions. Various reaction parameters, such as solvent type, catalyst ratio, catalyst concentration, temperature of catalyst formation and temperature of polymerization, were varied to determine the nature and degree of their effect on polymerization. This information was then applied to the polymerization of the block copolymers. The experimental methods employed for homopolymerization were the same as those of block copolymerization described below.

Block copolymer synthesis

A variety of high density polyethylene diblock copolymers were prepared for this study by modification of a previously reported synthesis of polybutadiene–polypropylene diblock copolymers[20,21]. Purification of reagents, handling and equipment design were as previously reported. *Table 1* lists the samples made for this study and the particular reaction conditions for each.

Molecular characterization

Basic information on all samples of this study was obtained by gel permeation chromatography (g.p.c.) and differential scanning calorimetry (d.s.c.). Detailed characterization by Fourier transform infra-red (*FT*i.r.) spectroscopy, dynamic mechanical thermal analysis (d.m.t.a.), thermogravimetric analysis (t.g.a.), high temperature g.p.c. and pyrolysis gas chromatography–mass spectrometry (g.c.–m.s.) on some of the samples was also carried out. From the detailed characterization of selected samples it was possible to develop simple methods based on d.s.c. and g.p.c. to determine the molecular weight and composition of the resultant block copolymers. These methods are discussed below.

The ambient g.p.c. work was done in toluene using near-monodisperse polybutadiene or polystyrene standards. High temperature g.p.c. was performed at 130°C in trichlorobenzene using polystyrene standards. D.s.c. reveals the characteristic transitions of the representative blocks and can also be used to determine the composition of the blocks in two ways. First, one can measure the heat capacity of the amorphous block relative to the total weight of block, and second, one can measure the heat of fusion of the polyethylene block relative to similarly made and treated homopolymer. Both of these methods assume that the characteristic behaviour of the polymers is unaffected by block copolymerization. This assumption has been shown to be quite valid based on comparison

Table 1 Summary of the synthesis of the samples used in this study

No.	Solvent	[Li] (10^3 mol l^{-1})	Li/Ti ratio	% Block A to A-*b*-B	% Block A in A-*b*-B	Weight polymer (g)/mole Ti ($\times 10^3$)
Polybutadiene-*b*-polyethylene						
133	Cyclohexane	4	1.65	40	25	11
134	Cyclohexane	2	1.85	30	35	12
135	Cyclohexane	3	2.60	23	20	13
136	Cyclohexane	3	2.90	20	25	6
137	Cyclohexane	2	1.65	38	25	29
138	Cyclohexane	1.5	1.90	6	50	5
141	Cyclohexane	1.2	1.80	n.d.	65	n.d.
142	Cyclohexane	1.5	2.25	n.d.	55	n.d.
143	Hexane	1.5	1.80	n.d.	55	n.d.
144	Cyclohexane	2	1.65	35	35	21
145	Cyclohexane	2	2.90	30	20	23
146	Hexane	2	1.95	35	45	14
147	Benzene	2.2	3.30	32	10	26
148	Benzene	2.5	4.70	26	20	28
149	Benzene	3.3	3.20	32	10	32
Polystyrene-*b*-polyethylene						
125	Cyclohexane	0.9	1.00	7	25	4
126	Benzene	1.1	1.75	8	30	5
127	Benzene	1.1	2.00	7	55	10
128	Cyclohexane	1.2	1.75	30	20	42
129	Cyclohexane	0.9	1.50	13	5	8
130	Cyclohexane	1.1	1.75	4	15	4
131	Cyclohexane	1.0	2.00	11	50	9

n.d., not determined

of composition determined more exactly by *FT*i.r. and pyrolysis g.c.–m.s. Lastly, d.m.t.a. was used to check for any anomalies and to give some estimation of the morphology and resultant mechanical behaviour. The general results of the characterization of the samples are contained in *Table 2*.

Morphological characterization

Most of the samples of this study were examined by transmission electron microscopy (TEM). Each was stained with either ruthenium or osmium tetroxide under different conditions, depending on the type and amount of each block. TEM and X-ray are perhaps the only ways to verify block structure in such materials. Characteristic microphase separation was observed in all samples, but in most cases the spacing and shape were distorted in contrast to typical expectations for amorphous–amorphous systems. Some samples were studied more thoroughly by TEM with regard to sample preparation. In some instances compression-moulded specimens of the same sample were processed in three different ways: (1) moulded at 160°C and quenched to 0°C, denoted as 'quenched'; (2) moulded at 160°C, quenched to 0°C and annealed at 120°C for 3 h under vacuum, denoted as 'quench/annealed'; and (3) moulded at 160°C, cooled slowly to 120°C (3–5°C $\min^{-1}$ on average), isothermal at 120°C for 20 min and then quenched to 0°C, denoted as 'slow cooled'. These three methods should give some indication of the morphology of the melt, the morphology of a highly nucleated/crystallized sample and the morphology of a system where crystallization is allowed to predominate, respectively.

Some of the samples were also subjected to both wide- and small-angle X-ray analysis. This analysis was performed on quenched films as well as on channel die (plane-strain compression) extruded/oriented pieces. The general results of the X-ray analysis and their implications with regard to the competition between phase separation

Table 2 Summary of the characterization of the samples used in this study

No.	M_n of block A	M_n(est.) of block B	T_g of block A (°C)	T_m of block B (°C)	ΔH block B (J/total wt)
Polybutadiene-*b*-polyethylene					
133	11 000	50 000	−94	134	140
134	16 000	180 000	−94	133	140
135	19 000	100 000	−93	132	125
136	21 000	75 000	−93	135	150
137	26 000	100 000	−91	133	150
138	38 000	50 000	−94	127	75
141	30 000	10 000	−90	125	15
142	30 000	10 000	−94	126	10
143	30 000	10 000	−93	123	30
144	32 000	70 000	−92	130	95
145	23 000	110 000	−91	133	110
146	23 000	50 000	−93	131	90
147	23 000	240 000	−90	135	145
148	21 000	100 000	−92	135	120
149	21 000	260 000	−92	135	160
Polystyrene-*b*-polyethylene					
125	60 000	180 000	89	137	115
126	40 000	80 000	94	132	110
127	70 000	60 000	98	133	80
128	40 000	350 000	96	135	130
129	40 000	350 000	100	134	135
130	40 000	230 000	100	137	130
131	45 000	45 000	95	135	100

and crystallization are discussed below. Details of the sample preparation, methods and results of the X-ray analysis will be published separately[59,60].

RESULTS AND DISCUSSION

Synthesis

More than 25 diblock copolymers were synthesized over the course of this study as well as more than 30 homopolymers. From the results of this work, a better picture of the factors that govern the effectiveness of this anionic to ZN transformation has emerged.

The results of the homopolymerization of ethylene using the n-BuLi/$TiCl_4$ catalyst systems are for the most part consistent with the findings of others[34–52] with one exception: a maximum in activity for the polymerization of ethylene in an alkane-based solvent occurs at a Li/Ti ratio of about 1.65 as opposed to about 2.125 for all the other solvents. The value of 1.65 is much closer to the theoretical value of 1.5 proposed by Siove and Fontanille[56] for the active species formed by reaction of n-BuLi and $TiCl_4$. This result also verifies the work of Friedlander[34] who more than 35 years ago demonstrated a similar effect. This suggests that there may be more than one active species formed by such a catalyst system, and that the aromaticity of the solvent is important particularly in the case of ethylene polymerizations. It should be noted that the association and reactivity of anions in various solvents is different, so that such a result is not unexpected. It is now generally accepted than n-BuLi exists as a hexamer in alkane solvents and a dimer in aromatic solvents. This affects not only the rate of reaction but also the degree of reaction. Thus, the ability of n-BuLi to alkylate and reduce titanium to the proper species should be a function of this association.

The information gained from the homopolymerization was useful for narrowing the conditions for optimum block copolymerization and for elucidating the importance of the association of the anion in the formation of an active catalyst. The results of the block copolymerizations can best be discussed by considering three 'measures' of the activity and efficiency of the reactions. The first measure is the amount of the anionic block that is converted to diblock copolymer. In other words, if 100 anionic chains are reacted with $TiCl_4$, how many of these will actually end up as block copolymer? This number, of course, is a function of reaction parameters and the maximum efficiency would be 33% if the active species proposed by Fontanille and co-workers[17–19] is formed. The results show that the most important factor in conversion of block A to diblock is the Li/Ti ratio. In general, the efficiency of conversion of the first block to diblock decreases as the Li/Ti ratio increases. This effect is most pronounced in the case of polybutadiene, which shows a higher efficiency of transformation relative to polystyrene. This effect may be related in part to the molecular weight differences, but generally for a given polymer the efficiency of transformation appears to be independent of molecular weight above some critical value. Instead, the difference exhibited between polystyrene and polybutadiene may arise from solubility and conformation variation of the resultant diblock as it is formed.

Once transformed, the living polymer–transition metal complex must effectively polymerize ethylene. This effectiveness will partly determine the overall diblock composition as well as the total yield. The overall diblock composition is also greatly influenced by other reaction parameters as seen in *Figure 1*. A distinct increase in the percentage of first block in the final diblock is observed as a function of both an increase in the Li/Ti ratio and the molecular weight of the first block. Again, very little effect is seen by varying the nature of the solvent. There does appear, however, to be some decrease in the first block content as the overall catalyst concentration is increased.

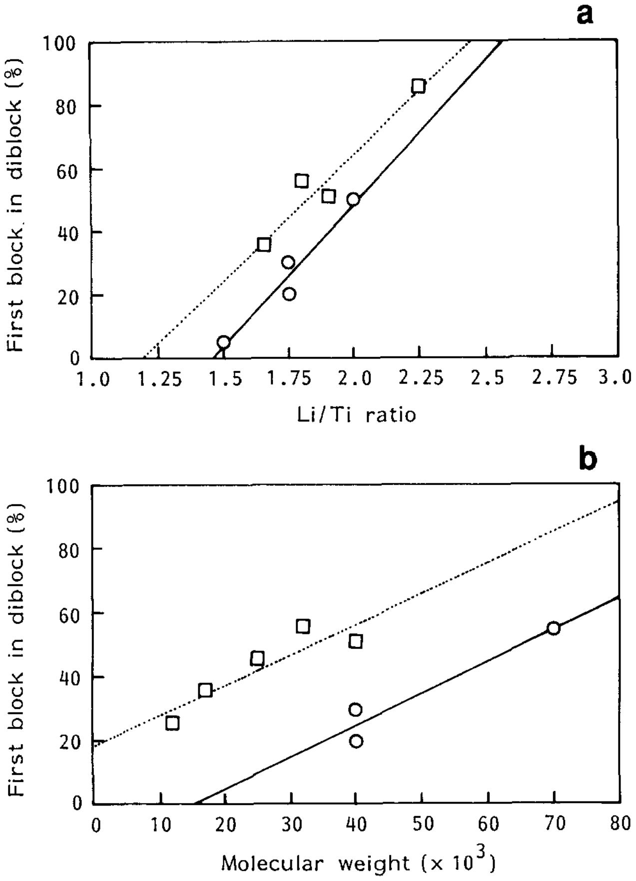

Figure 1 Composition of the final diblock as a function of (a) Li/Ti catalyst ratio (M_w = 30 000–40 000) and (b) the molecular weight of block A (Li/Ti ratio = 1.6–1.8). ○, Polystyrene; □, polybutadiene

The amount of first block transformed and the ability to polymerize polyethylene determines the overall yield of polymer. For this reason, a maximum in yield is observed as a function of the Li/Ti ratio. Most noteworthy is the observed maximum at a Li/Ti ratio of about 1.65, consistent with the homopolymerization of polyethylene by a n-BuLi/$TiCl_4$ catalyst in an alkane. It should be noted, however, that the yields in the case of diblock are two to four times greater than the corresponding similar homopolymerization case. This clearly demonstrates improvement in catalytic activity as the molecular weight of the 'alkylating' species is increased and the solubility of the catalyst improved.

Characterization

Molecular characterization of the resultant diblock copolymers is consistent with the chemical composition and two-phase structure of block copolymers. D.s.c. shows the presence of two distinct phases and gives a

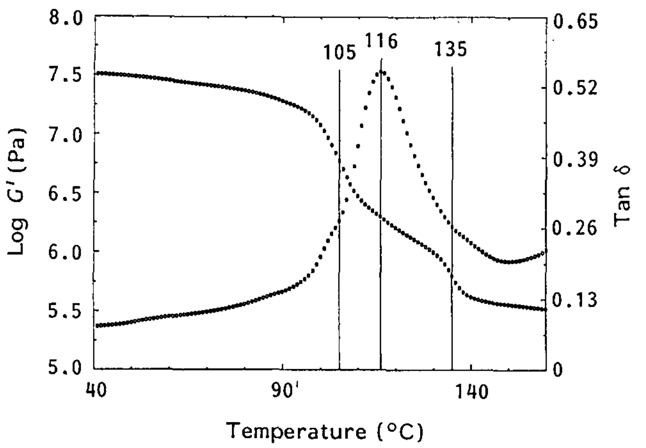

Figure 2 Dynamic mechanical response of a polystyrene-*b*-polyethylene copolymer under shear

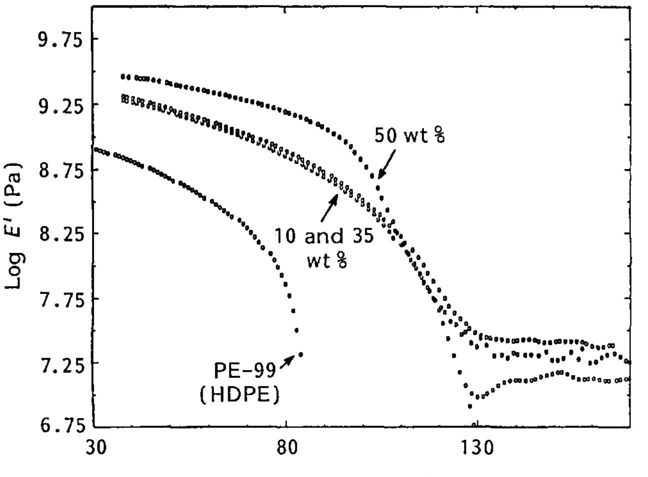

Figure 3 Dynamic mechanical analysis of polystyrene-*b*-polyethylene copolymer as a function of block A content

good indication of the relatively high linearity and crystallinity of the high density polyethylene (HDPE) phase. Overall, the d.s.c. results are consistent with typical block copolymer behaviour, with little indication of the effect of crystallization on the phase behaviour.

Dynamic mechanical analysis is also consistent with the block copolymer structure, and gives an indication of the overall composition and morphology. *Figure 2* is a typical example of a polystyrene-*b*-polyethylene diblock under shear. In tension, the glass transition of the polystyrene and the onset of melting of the polyethylene overlap and are not as well separated.

Modulus temperature curves, such as those in *Figures 3* and *4*, are useful in giving a qualitative indication of the relative proportions of the phases. In the case of the polystyrene-*b*-polyethylene system, as the percentage of polystyrene in the diblock increases, an initial increase in room temperature modulus is observed. These materials are considerably stiffer at elevated temperatures compared to similarly made HDPE homopolymer. The fact that the curves show little change once more than 25–35% polystyrene content is reached is an indication of a constant structure over a wide composition. This is uncharacteristic of amorphous diblocks but consistent with recent experimental results and theoretical predictions[11–14,61,62]. This point will be discussed further in the TEM analysis and in relation to the composition–morphology behaviour exhibited by this system.

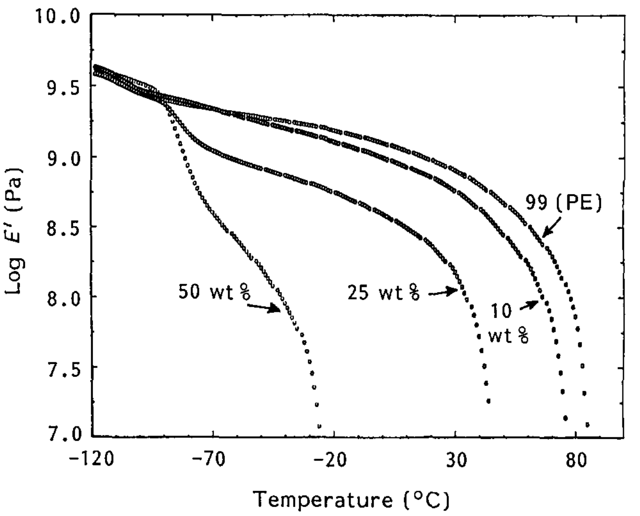

Figure 4 Dynamic mechanical analysis of polybutadiene-*b*-polyethylene copolymer as a function of block A content

The polybutadiene-*b*-polyethylene materials also show interesting dynamic mechanical spectra, which are different from those of the polystyrene-based systems. Most of this difference arises from the much lower glass transition and modulus of polybutadiene relative to polystyrene. Changes in block composition for the polybutadiene-*b*-polyethylene system appear more like the case of traditional amorphous blocks and are consistent with the electron microscopy results as well.

TEM is perhaps the most direct way to prove block copolymer structure owing to the unique microphase separation exhibited by such materials. *Figures 5* and *6* show the typical structure of HDPE homopolymer and a polystyrene-*b*-polyethylene diblock copolymer. In the quenched state (*Figures 5b* and *6b*) the resultant morphology is analogous to that typical of amorphous diblock copolymers, except for the fact that a perturbed spherical or platelet-type morphology exists over a wide compositional range. In most cases, however, the morphology consists of uniform, well dispersed polystyrene particles in the 30 nm size range. The quenched state is a good approximation of the morphology in the melt even though polyethylene still crystallizes. The level and size of the polyethylene crystallites are small and thus do not tend to disrupt the overall morphology. Annealing a previously quenched sample allows the extent of crystallization to be maximized by perfecting the large number of small crystallites. This results in perturbation of the morphology (*Figures 5c* and *6c*). At lower magnifications, a cross-hatched, spherulitic textured morphology becomes apparent (*Figures 5d* and *6d*), although it is not nearly as distinct as that of the HDPE homopolymer. Slow cooling a sample directly from the melt gives a morphology almost identical to the quench/annealed sample, since the rate of polyethylene crystallization is quite high in these materials. Overall, it appears that either phase is perturbed by the existence of the other and the level of perturbation depends on the block composition.

The polybutadiene-*b*-polyethylene materials also exhibit morphologies more complex than traditional amorphous

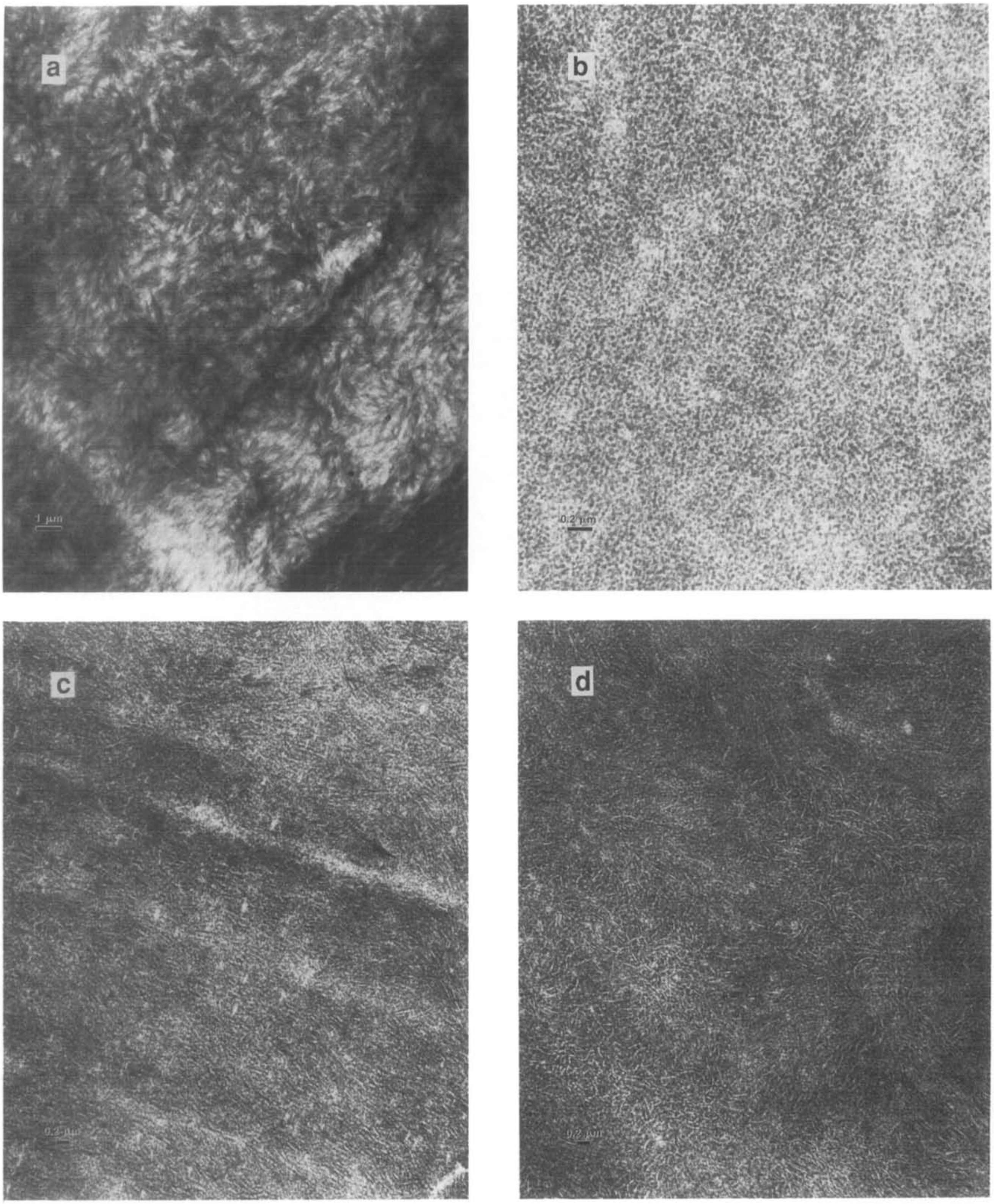

Figure 5 Transmission electron micrographs of (a) HDPE and a 30 wt% polystyrene copolymer: (b) no. 126 quenched; (c) no. 126 annealed; (d) no. 126 slow cooled

diblocks but different to those containing polystyrene. *Figure 7* shows two diblocks each containing about 25 wt% of polybutadiene. The fine dispersion of the polybutadiene phase is greatly changed by annealing of a quenched sample, and the spherulitic texture of the polyethylene appears to dominate. The polybutadiene microdomains appear to divert the crystallizing front or in some cases are ruptured by it. Since the crystallization of the polyethylene is occurring well above the glass transition of the polybutadiene phase, rupture of the polybutadiene domains seems quite plausible in comparison to such behaviour in the case of polystyrene. As the percentage of polybutadiene is increased, a co-continuous structure appears (*Figure 8*) and eventually

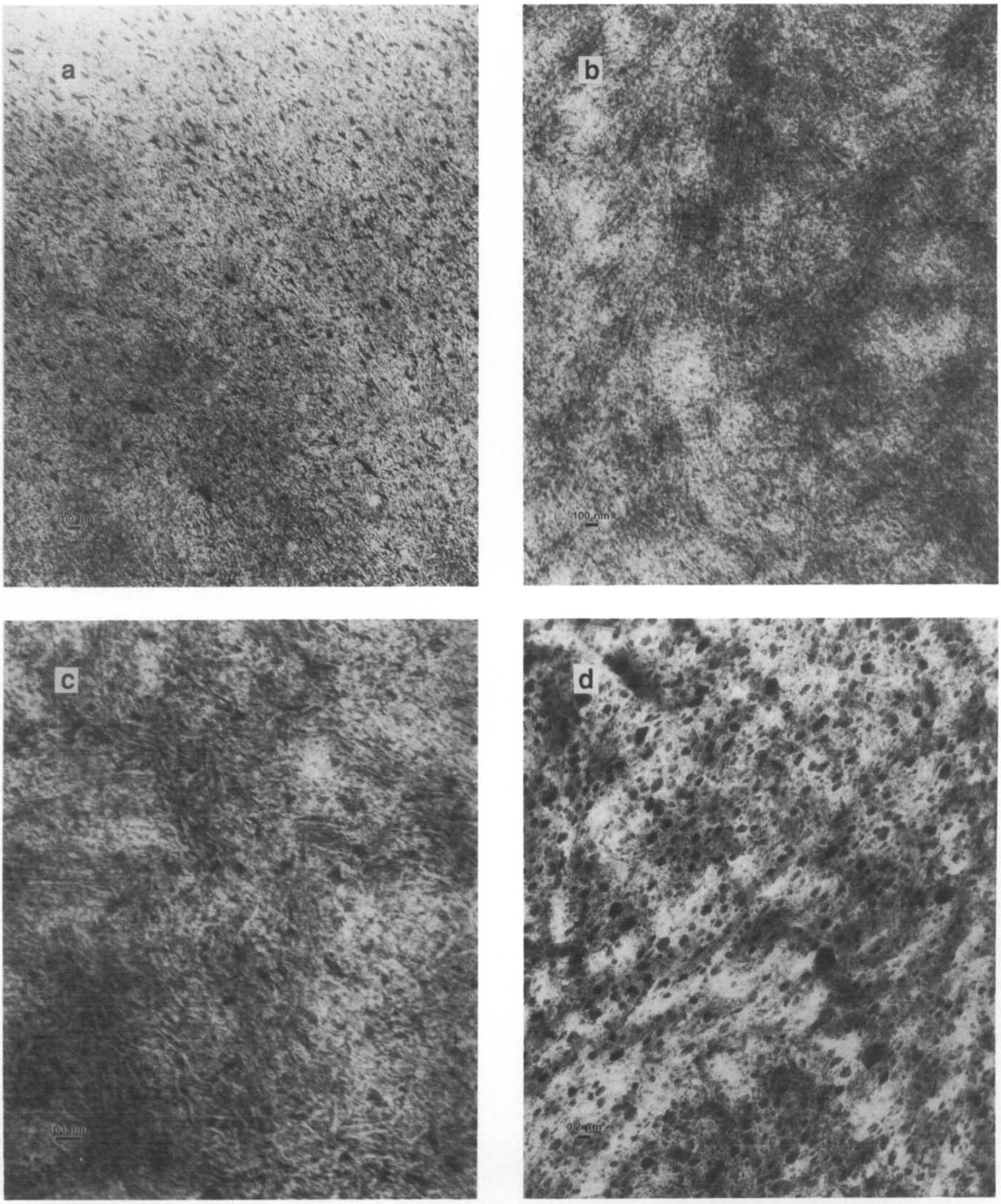

Figure 6 Transmission electron micrographs of a 50 wt% polystyrene copolymer (no. 131): (a) quenched; (b) quenched; (c) annealed; (d) annealed

inversion occurs to give a polybutadiene matrix and a polyethylene dispersed phase (*Figure 9*).

The composition–morphology relationship seen in the polybutadiene-*b*-polyethylene system is more typical of traditional amorphous diblock systems than is the case for polystyrene-*b*-polyethylene. This is most likely due to the deformability of the polybutadiene phase relative to polystyrene. The assumption that both systems are phase separated in the melt and crystallize upon cooling appears to be a good one. However, since crystallization of the polyethylene occurs very near the glass transition of the polystyrene and well above that of the polybutadiene, different morphologies can be expected to result. Thus, polystyrene may place more constraint on the polyethylene

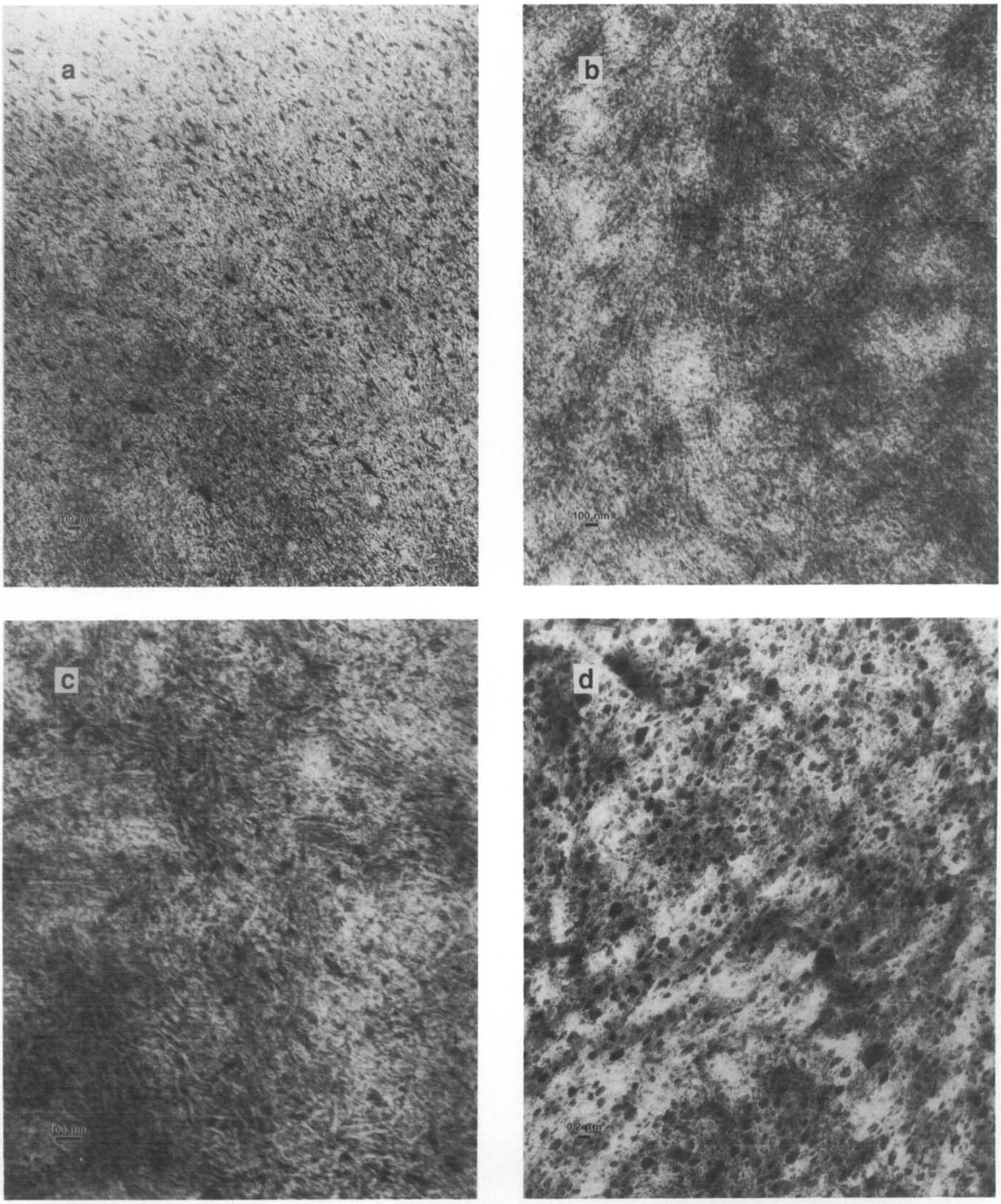

Figure 7 Transmission electron micrographs of various 25 wt% polybutadiene copolymers: (a) no. 137 quenched; (b) no. 137 annealed; (c) no. 137 annealed; (d) no. 136 annealed

than polybutadiene. This difference appears not to have been considered by recent theories regarding crystallization in diblock copolymers.

The DiMarzio–Guttman–Hoffman (DGH)[61] and the Whitmore–Noolandi (WN)[62] theories both assume that the equilibrium morphology of a crystallizable diblock is lamellar at all volume fractions. Inherent in both of these theories, however, is the assumption that the material forms a one-phase melt such that the two processes of crystallization and phase separation compete. This competition leads to a final structure which is lamellar with regards to phase separation and a slightly

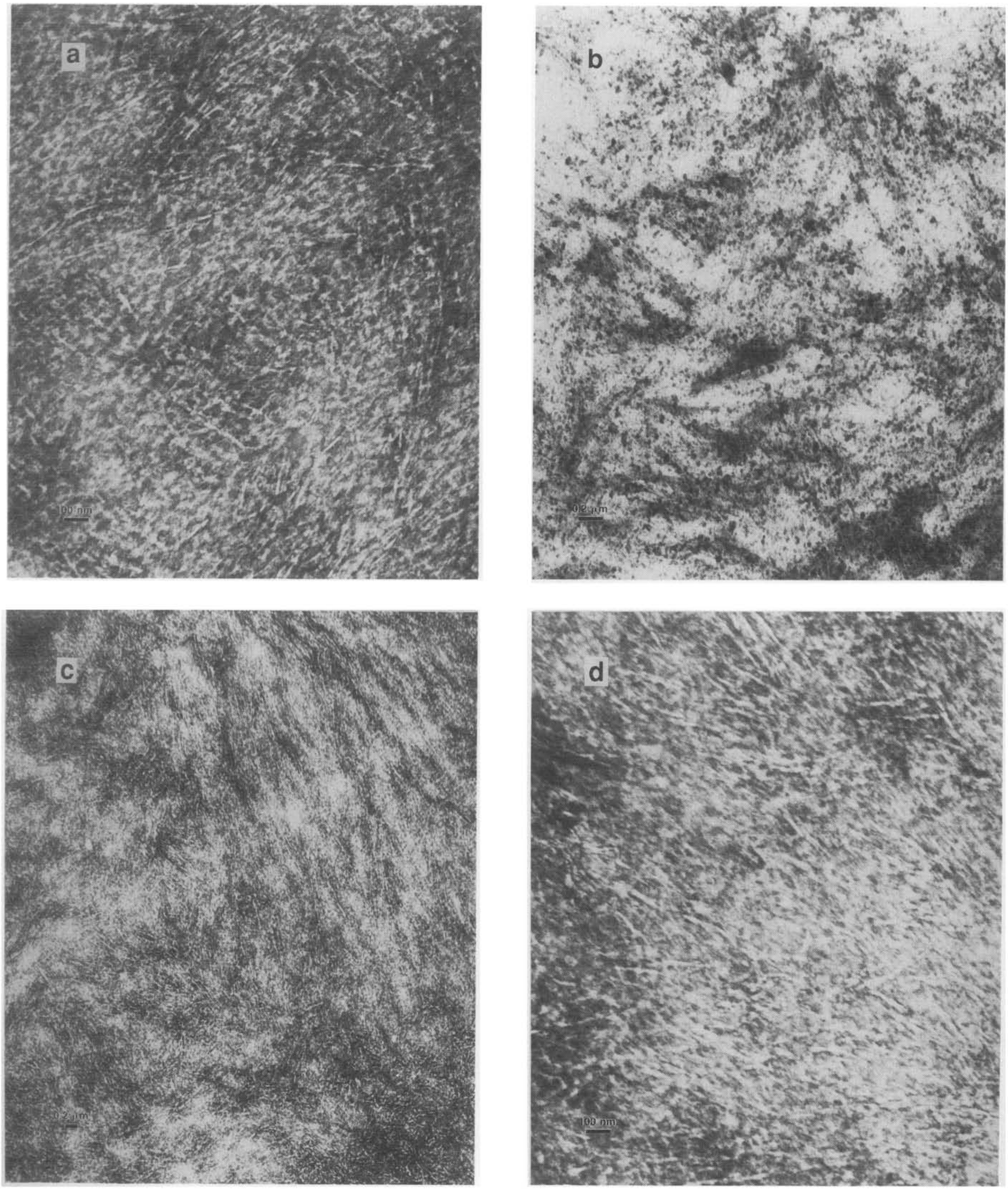

Figure 8 Transmission electron micrographs of high polybutadiene copolymers: (a) 35 wt% quenched; (b) 35 wt% annealed; (c) and (d) 50 wt% annealed

compressed, chain-folded crystalline structure within the crystallizable block. It seems apparent that a two-phase melt may not necessarily result in a lamellar structure, and that the 'strength' of this two-phase structure relative to the energetics of crystallization should influence the final morphology. Thus, the results presented here are consistent with these views.

Recent experimental verification of the DGH and WN theories[11–14] has been carried out with polyethylene diblocks containing rubbery second blocks. Such systems may allow one to come closer to true equilibrium and thus match theory. A glassy second block, however, may lock in a metastable structure and thus not follow theory. This behaviour is analogous to the wide morphological

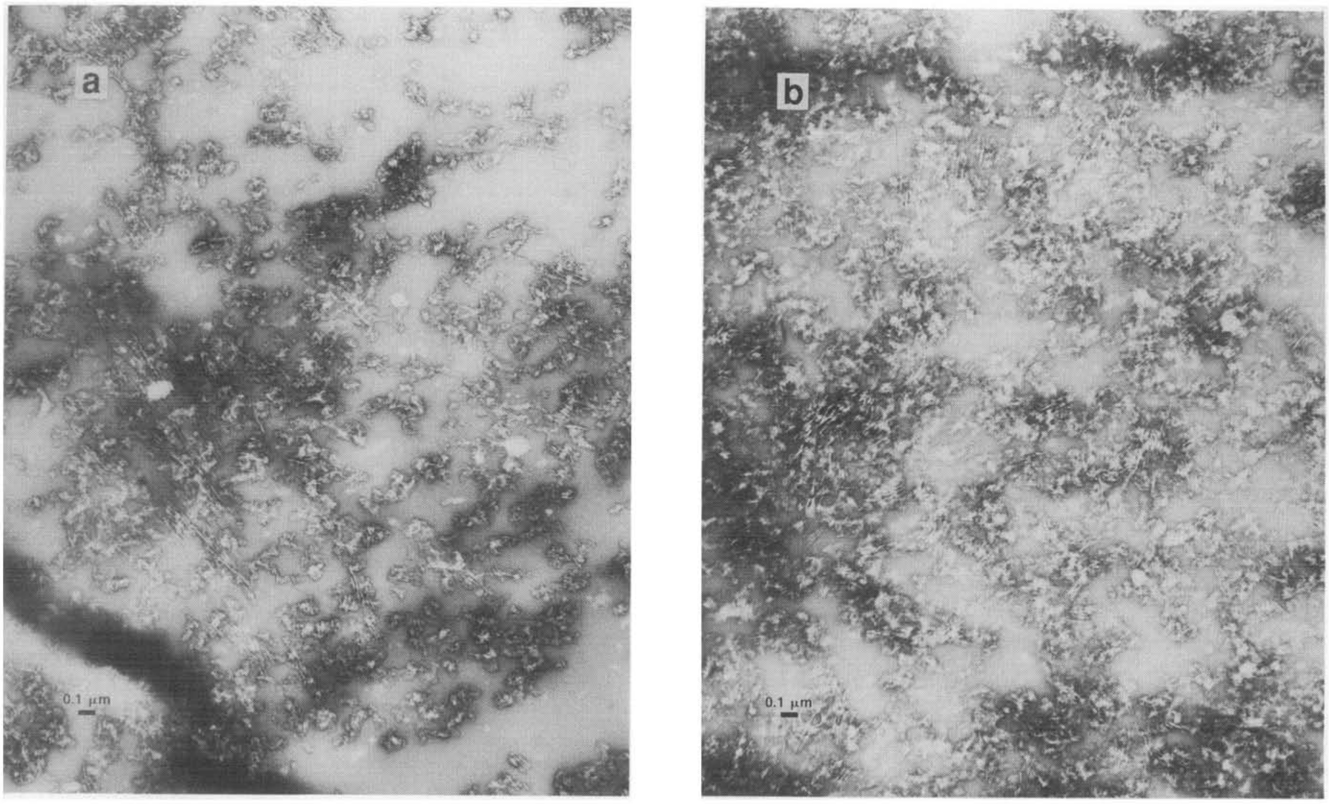

Figure 9 Transmission electron micrographs of a 65/35 wt% polybutadiene-*b*-polyethylene copolymer (no. 141): (a) quenched; (b) annealed

variations displayed with amorphous diblocks solution-cast from different types of solvents. The recent experimental work on crystallizable diblocks has also provided two interesting points. First, the processing history of the materials becomes extremely important in light of the fact that there are now two kinetic and two thermodynamically driven processes competing within one material, thus it is possible to prepare two quite different morphologies and obtain different properties from the same material. Second, since crystallization can occur from either a one-phase or two-phase melt, the nature of the crystallization can also be greatly affected. In cases where crystallization occurs from a homogeneous melt, classical nucleation and growth processes are observed, which lead to conventional chain folding such that the folds are at the phase-separated surfaces and the chains are roughly normal to these surfaces. In some cases, however, crystallization from a two-phase melt places a topological constraint on the crystallizing chain such that the folds lie along the surfaces and the chains crystallize parallel to the phase-separated surface. Such an argument was theorized[9] and recently confirmed experimentally[11–14,59,60].

Crystallization of polymers from small molecules is unique in that there is an associated high end surface free energy associated with the process arising from the unique nature of the crystal–melt interface. This is due to the restricted conformation of the chains imposed by a locally high chain density, the closeness of two crystallizing surfaces, as well as inter- and intramolecular interactions. This locally high energy can be dissipated by chain termination or folding. Thus, the end surface free energy is related to the number of chain ends and folds present at the surface. Ideally, the free surface of a polymer crystal will contain only chain ends, folds and chains parallel to the surface so as to minimize the local free energy. Therefore it seems reasonable to assume that as chain folding increases, the surface free energy decreases[63]. Conversely, the more regular (smooth) the surface, the lower the surface free energy, resulting in a higher degree of chain folding.

Since the surface free energy determines the crystal shape and the overall nucleation and growth mechanism, block copolymerization can be assumed to have a significant influence on the nature of the crystallization process. Furthermore, the rate of crystallization is governed by the deposition of the folded chain nuclei onto the crystal substrate (i.e. phase-separated surface). The remainder of the chain must then crystallize sequentially in register with this substrate or surface. Thus this process becomes a function of the surface roughness and the local free energy which is inherently minimized in a phase-separated block copolymer system. In a block copolymer, the crystal and amorphous phases can be joined at a common interface and the nucleation and growth of the crystal predetermined by the nature of the phase separation. Therefore, in the case of crystallization from a two-phase melt, the microphase-separated surface and interface effectively eliminate chain ends by pre-aligning them at a surface. This in turn diminishes the local surface free energy and promotes chain folding. This situation is analogous to epitaxial growth on an oriented surface[7]. This type of 'orientation-induced nucleation' is common in stressed systems where some degree of alignment of the molecules reduces the need for arrangement prior to crystallization[8]. Such alignment occurs with the chain axis lying along the surface plane. Surfaces which do not show this orienting effect do not exhibit epitaxy. In block copolymers, alignment, adsorption and orientation are inherent to the microphase-separated morphology. In addition, surface nucleation and growth in a geometrically constrained environment such as a block copolymer can lead to crystal growth with the chain axis parallel to the surface, with the fastest rate of growth normal to the surface in order to minimize the free energy.

Overall, the richness of the variable morphologies attainable from crystallizable block copolymers makes them ideal candidates for study as well as key materials for new applications. Since such diblock copolymers can be made to have lamellar phase morphologies in which one phase is crystalline and oriented normal to the surface, a uniquely anisotropic reinforced material can be produced. Future work is aimed at better understanding the nature of crystallization in these types of materials and ascertaining the molecular parameters that lead to the best reinforced morphology.

ACKNOWLEDGEMENTS

The technical assistance of Mr Donald Bachert (synthesis) and Ms Nancy Dudash (microscopy), along with the permission of EniChem management to publish this work, is gratefully acknowledged.

REFERENCES

1 Lock, G. *Am. Chem. Soc. Polym. Prepr.* 1985, **26**, 60
2 Prabhu, P., Theil, M. H. and Gilbert, R. D. *J. Polym. Sci., Polym. Lett. Edn* 1980, **18**, 389
3 Prabhu, P., Theil, M. H. and Gilbert, R. D. *J. Polym. Sci., Polym. Chem. Edn* 1983, **19**, 523
4 Takahashi, T., Mizuno, H. and Thomas, E. L. *J. Macromol. Sci., Phys.* 1983, **B22**, 425
5 Buscio, V., Corradini, P. and Savino, V. *Makromol. Chem. Rapid Commun.* 1984, **5**, 737
6 Boor, J. Jr 'Ziegler-Natta Catalysts and Polymerizations', Academic Press, New York, 1979
7 Wunderlich, B. 'Macromolecular Physics', Academic Press, New York, 1980
8 Binsberger, F. *J. Polym. Sci., Polym. Symp. Edn* 1977, **61**, 11
9 Drzewinski, M. ScD Thesis, Massachusetts Institute of Technology, 1986
10 Drzewinski, M. *Polym. Mater. Sci. Eng.* 1985, **53**, 113
11 Douzinas, K. C., Cohen, R. E. and Halasa, A. F. *Macromolecules* 1991, **24**, 4457
12 Douzinas, K. C. and Cohen, R. E. *Macromolecules* 1992, **25**, 5030
13 Register, R. *Am. Chem. Soc. Polym. Prepr.* 1992, **33**, 424
14 Rangarajan, P., Register, R. and Fetters, L. *Macromolecules* 1993, **26**, 4640
15 Richards, D. *Br. Polym. J.* 1980, **12**, 89
16 Richards, D., Cohen, P., Abadie, M. J. M. and Schue, F. *Polymer* 1981, **22**, 1316
17 Siove, A. and Fontanille, M. *Makromol. Chem.* 1980, **181**, 1815
18 Siove, A. and Fontanille, M. *Eur. Polym. J.* 1981, **17**, 1175
19 Soum, A., Siove, A. and Fontanille, M. *J. Appl. Polym. Sci.* 1983, **28**, 961
20 Drzewinski, M. and Cohen, R. *J. Polym. Sci., Polym. Chem. Edn* 1986, **24**, 2457
21 Drzewinski, M. *Polym. Mater. Sci. Eng.* 1985, **52**, 437
22 Szwarc, M. 'Carbanions, Living Polymers and Electron Transfer Reactions', Wiley Interscience, New York, 1968
23 Flory, P. 'Principles of Polymer Chemistry', Cornell Press, New York, 1957
24 Natta, G., Pino, P. and Peraldo, M. *J. Polym. Sci.* 1957, **26**, 120
25 Natta, G., Pino, P. and Giannini, U. *J. Inorg. Nucl. Chem.* 1958, **8**, 612
26 Natta, G. and Pasquon, I. *Adv. Catal.* 1959, **11**, 1
27 Natta, G., Corradini, P. and Bassi, I. W. *J. Am. Chem. Soc.* 1965, **80**, 755
28 Zambelli, A., Giongo, M. G. and Natta, G. *Makromol. Chem.* 1968, **112**, 183
29 Zambelli, A., Sacchi, M. C., Locatelli, P. and Zannoni, G. *Macromolecules* 1980, **13**, 798
30 Fink, G. and Rottler, R. *Angew. Makromol. Chem.* 1981, **94**, 25
31 Fink, G., Rottler, R., Schell, D. and Zoller, W. *J. Appl. Polym. Sci.* 1976, **20**, 2779
32 Zambelli, A., Sacchi, M. C., Locatelli, P. and Zannoni, G. *Macromolecules* 1982, **15**, 211
33 Zambelli, A., Sacchi, M. C., Locatelli, P. and Tritto, I. *Macromolecules* 1982, **15**, 831
34 Friedlander, H. *Ind. Eng. Chem.* 1957, **49**, 1885
35 Badische Aniline & Soda-Fabrik Aktiengesellschaft, British Patent no. 796,912, 1958
36 Ludlum, D., Anderson, A. and Ashby, C. *J. Am. Chem. Soc.* 1958, **80**, 1380
37 Frankel, M., Rabani, J. and Zilkha, A. *J. Polym. Sci.* 1958, **28**, 387
38 Kocheskov, K., Kargin, V., Puljev, O. and Sogolova, T. *J. Polym. Sci.* 1959, **34**, 121
39 Jones, M., Martius, U. and Thorne, M. *Can. J. Chem.* 1960, **38**, 2303
40 Evans, A. and Owen, G. *J. Chem. Soc.* 1961, 1733
41 Solomon, O., Dimone, M., Amrozh, K. and Tomesku, M. *J. Polym. Sci.* 1961, **52**, 205
42 Korotkov, A. *Vysokomol. Soed* 1961, **4**, 10
43 Tsou, K., Megee, J. and Maltesta, A. *J. Polym. Sci.* 1962, **58**, 229
44 Heller, J., Tieszan, D. and Parkinson, D. *J. Polym. Sci. A* 1963, **1**, 125
45 Hopkins, E. and Miller, M. *Polymer* 1963, **4**, 75
46 Cooper, W. *Rubber Plast. Age* 1963, 44
47 Hopkins, E. and Miller, M. *Polymer* 1964, **5**, 432
48 Lehr, M. and Moyer, P. *J. Polym. Sci. A* 1965, **3**, 231
49 Calderon, N. Belgian Patent no. 698,075, 1967
50 Wang, J. and Menapace, H. *J. Org. Chem.* 1968, **33**, 3794
51 Zilkha, A., Calderon, N., Ottolenghi, A. and Frankel, M. *J. Polym. Sci.* 1959, **40**, 149
52 Boor, J. Jr *Macromol. Rev.* 1967, **2**, 115
53 Aldissi, M. *J. Chem. Soc. Commun.* 1984, 1347
54 Amass, A., Bas, S., Gregory, D. and Mathew, M. *Makromol. Chem.* 1985, **186**, 325
55 Galvin, M. and Wnek, G. *Polym. Bull.* 1985, **13**, 109
56 Siove, A. and Fontanille, M. *J. Polym. Sci., Polym. Chem. Edn* 1984, **22**, 3877
57 Cansell, F., Siove, A. and Fontanille, M. *Makromol. Chem.* 1985, **186**, 379
58 Zhang, X. *Makromol. Chem.* 1990, **191**, 1765
59 Drzewinski, M., Bellare, A. and Cohen, R. *Macromolecules* 1994, **27**, 2321
60 Drzewinski, M. and Register, R. unpublished results
61 DiMarzio, E., Guttman, C. and Hoffman, J. *Macromolecules* 1980, **13**, 1194
62 Whitmore, M. and Noolandi, J. *Macromolecules* 1988, **21**, 1482
63 Ashman, P. and Booth, C. *Polymer* 1975, **16**, 889